energies

MDPI

Article

Compact Thermal Modeling of Power Semiconductor Devices with the Influence of Atmospheric Pressure

Paweł Górecki

Department of Marine Electronics, Gdynia Maritime University, 81-225 Gdynia, Poland; p.gorecki@we.umg.edu.pl

Abstract: The efficiency of the heat dissipation process generated in semiconductor devices depends on many factors, related both to the parameters of the cooling system and environmental factors. Regarding the latter factors, ambient temperature and volume in which the device operates are typically indicated as the most important. However, in the case of the operation of semiconductor devices in non-standard conditions, e.g., in stratospheric airships, the thermal parameters of the device are significantly affected by a low value of atmospheric pressure. This paper presents a compact thermal model of a semiconductor device, considering the effects of reduced atmospheric pressure along with its experimental verification under various cooling conditions, thus obtaining high compliance for computation and measurement results. The formulated model is dedicated to circuit-level simulations, and it enables computations of the junction temperature of the semiconductor device in a short time. It is also shown that lowering atmospheric pressure can double the value of the junction-ambient thermal resistance.

Keywords: thermal model; thermal impedance; power semiconductor devices; stratosphere; airship

Citation: Górecki, P. Compact Thermal Modeling of Power Semiconductor Devices with the Influence of Atmospheric Pressure. *Energies* **2022**, *15*, 3565. https://doi.org/10.3390/en15103565

Academic Editor: Abu-Siada Ahmed

Received: 8 April 2022
Accepted: 11 May 2022
Published: 12 May 2022

1. Introduction

In recent years, near-space, including the stratosphere, has been an area of great interest for scientists from all over the world, especially in the field of solar-powered stratospheric airship design. These airships are intended to carry large payloads (about 1000 kg) to the stratosphere (at altitudes around 20 km) for several months. Potentially, they can be used in civilian areas, such as telecommunications, land observation, mapping, travel and military areas, e.g., coastal surveillance [1,2].

In order to meet the expectations of high endurance, the energy system typically consists of solar panels, lithium batteries, fuel cells and electronic control systems [3,4]. In numerous papers, selected problems of such a system were analyzed, and in particular, these related to thermal phenomena in the components of this system. These phenomena are of particular importance because they influence both characteristics of semiconductor devices [5] and their reliability [6].

Computer simulations are an important stage in the design of electronic circuits. One of the most popular tools used to perform such simulations is SPICE (Simulation Programme with Integrated Circuits Emphasis). SPICE is a general-purpose, open-source circuit-level simulator dedicated to analog electronics. This program is commonly used in integrated circuit and PCB-level design to check their integrity and to predict circuit behavior.

One of the main goals of computer simulations is the selection of system components that allow it to work reliably. To achieve this, it is necessary to consider thermal phenomena in computations. The models embedded in the SPICE program omit these phenomena; therefore, the literature contains numerous compact thermal and electrothermal models that allow for the determination of the junction temperature of both transistors and diodes. However, none of these models consider the influence of reduced atmospheric pressure on the thermal properties of semiconductor devices.

However, this does not mean that there are no models of other components and systems operating under reduced pressure in the literature. Such models are formulated using, e.g., the finite element method. Unfortunately, models formulated in this way are not compatible with circuit-level simulation programs, which makes them difficult to use in the design of electronic circuits [7].

Daia et al. [8] focused on determining temperature distribution on the surface of the photovoltaic array and the airship envelope and its change during the day due to variable insolation and wind occurring in the stratosphere. The remaining components of the energy system were omitted from their analysis. The authors of [9] achieved a similar goal, but one temperature value was computed for the entire photovoltaic panel.

Zhang et al. [10] analyzed changes in gas temperature inside an airship balloon and an airship shell with natural convection and external forced convection. Unfortunately, their analysis does not consider thermal phenomena occurring in the energy system.

Li et al. [11] focused on examining the influence of stratospheric operating conditions on the efficiency of photovoltaic panels placed on an airship's surface. Unfortunately, in their analysis, they omitted the energy conversion systems, which are a necessary integrating component between the photovoltaic array and the load [12].

As mentioned above, the components of the energy system also include lithium batteries. The authors of [3,13] focused on the analysis of the operation of these components in a stratospheric airship. However, in the case of these batteries, no thermal analyses were performed, which, as shown in [14], affect the properties of such a system operating on the Earth's surface.

On the other hand, Elsayedab et al. [15] presented a thermal model of a grilled heat sink dedicated to electronic components along with its experimental verification carried out in a wide range of changes in atmospheric pressure. The model was formulated using the finite element method (FEM), which makes it incompatible with peripheral analysis environments popular among designers of electronic circuits. The determination of all of the values of the parameters of the elements of the heat flow path of the model formulated with the use of FEM, in particular regarding the radiation and convection of heat from individual materials, is also a serious problem.

Nevertheless, in all the articles mentioned above on electronics operating in low pressure environments, thermal phenomena in semiconductor devices were omitted. These devices play a key role in both power converters converting energy generated by the photovoltaic array and the lithium battery charging control systems occurring in the stratospheric airships mentioned before. These circuits are constructed using both low and high-power semiconductor devices. The designers of these systems, in order to characterize the thermal properties of semiconductor devices and to simultaneously consider their cooling system in a thermally steady state, typically use junction-ambient thermal resistance R_{thj-a}, and in order to characterize thermal transients, the junction-ambient transient thermal impedance Z_{thj-a} *(t)* is defined by the formula [16,17]

$$Z_{thj-a}(t) = \frac{T_j(t) - T_a}{p_{th}} \tag{1}$$

where $T_j(t)$ is the junction temperature waveform, T_a is the ambient temperature and p_{th} is the value of the step of the power dissipated in the tested device.

The thermal resistance R_{thj-a}, which is the value of $Z_{thj-a}(t)$ in a steady state, strongly depends on many factors related both to the design of the cooling system and operating conditions of the system. The most significant factors related to the design of the cooling system are the dimensions of the heat sink, the material which it was made of, the use of fans, and the use of thermal grease [18]. Ambient temperature, the junction temperature of the device and air movement in the volume in which the device is placed [19,20] are examples of the most significant factors describing the operating conditions of the system. However, the dependence of junction-ambient thermal resistance on atmospheric pressure has not been investigated so far.

The junction temperature of the semiconductor device in a thermally steady state depends on the value of the thermal resistance R_{thj-a}, and the reliability of the designed system depends on it in a key way [6,21]. Therefore, knowledge of the dependence of thermal resistance R_{thj-a} on atmospheric pressure is of particular importance for the design of electronic systems operating in conditions of lowered atmospheric pressure, e.g., in the stratosphere. By analyzing the properties of convection in the heat transfer process, it can be seen that its efficiency depends on atmospheric pressure. This is due to a decrease in a mass of air of constant volume with a decrease in pressure in this volume. The mentioned decrease in efficiency should be visible in the course of transient thermal impedance $Z_{thj-a}(t)$ and in particular in thermal resistance R_{thj-a}.

This article presents a new, non-linear compact thermal model of a semiconductor device that considers the influence of atmospheric pressure on the course of its thermal impedance $Z_{thj-a}(t)$. This model is dedicated to circuit-level simulations in the SPICE program. Section 2 presents the form of the model, Section 3 describes the measurement set-up for experimental verification and Section 4 presents the results of experimental verification along with the discussion.

2. Form of the Model

The formulated non-linear compact thermal model of a semiconductor device has the form of a circuit and is dedicated to the SPICE program. In this model, all mechanisms and paths of heat transfer from the semiconductor chip to the surroundings are considered. The circuit representation of the model is shown in Figure 1.

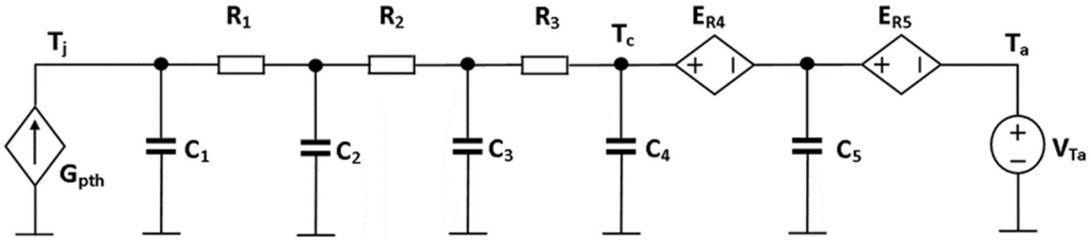

Figure 1. Circuit representation of the formulated thermal model.

The structure of the presented model is based on the classic linear Cauer RC thermal model; however, the influence of the device junction temperature is considered (the ambient temperature and atmospheric pressure on thermal resistances occurring in the heat flow paths from the semiconductor chip to the surroundings). The structure of the formulated model is an electrical analog of the heat transfer equation [22]. In the formulated model, the voltage in node T_j is equal to the junction temperature, whereas the source V_{Ta} models the ambient temperature T_a. The temperature values of the individual elements of the heat flow path are represented by voltages in individual nodes. The power dissipated in the semiconductor device is modelled by controllable current source G_{pth}, and the thermal resistances of each element of the heat flow path are represented by resistors R_1, R_2 and R_3, which are responsible for modeling thermal resistances on the way from the junction to the case and to the controllable voltage sources E_{R4} and E_{R5}, which model thermal resistance on the way from the case to the surroundings. The output value of each source E_{Ri} is described with the following equation:

$$E_{Ri} = d_i \cdot i_{ERi} \cdot \left(R_{th2} \cdot exp\left(-\frac{p - p_0}{p_z} \right) + R_{th1} \cdot (1 - a \cdot (T_a - T_0)) \cdot exp\left(-\frac{T_j - T_a}{T_z} \right) + R_{th0} \cdot (1 - b \cdot (T_a - T_0)) \right) \quad (2)$$

In Equation (2), R_{th0} is the minimum value of the thermal resistance at $T_a = T_0$. R_{th1} represents the maximum change in the value of the thermal resistance while changing the device junction temperature and $T_a = T_0$. R_{th2} is the coefficient describing the dependence of thermal resistance on atmospheric pressure. Coefficients a and b are ambient temperature rates of change in thermal resistance, whereas T_z determines the slope of dependence

$R_{th}(T_j)$, and p_z is the slope of dependence $R_{th}(p)$. i_{ERi} is the current of source E_{Ri}, and d_i is the quotient of the thermal resistance of the ith element of the heat flow path and the semiconductor device thermal resistance R_{th}. The presented form of (2) is formulated by the author on the basis of the described in literature [23] dependences of heat flux on the gradient of temperature (heat conduction), on differences between the temperature of the cooled surface and the ambient temperature (heat convection) and on the absolute temperature (heat radiation) and the nonlinear compact thermal model presented in [20].

Thermal capacities in the heat flow path are marked by C_1–C_5. Thermal capacities slightly depend on temperature [24] and pressure; therefore, the values of thermal capacities are constant in the formulated model.

3. Measurement Set-Up

In order to investigate the influence of atmospheric pressure on the thermal properties of a diode, its transient thermal impedance $Z_{thj-a}(t)$ was measured. To achieve this goal, the following measurement set-up based on the one presented in [25] was used. The diagram of this set-up is shown in Figure 2.

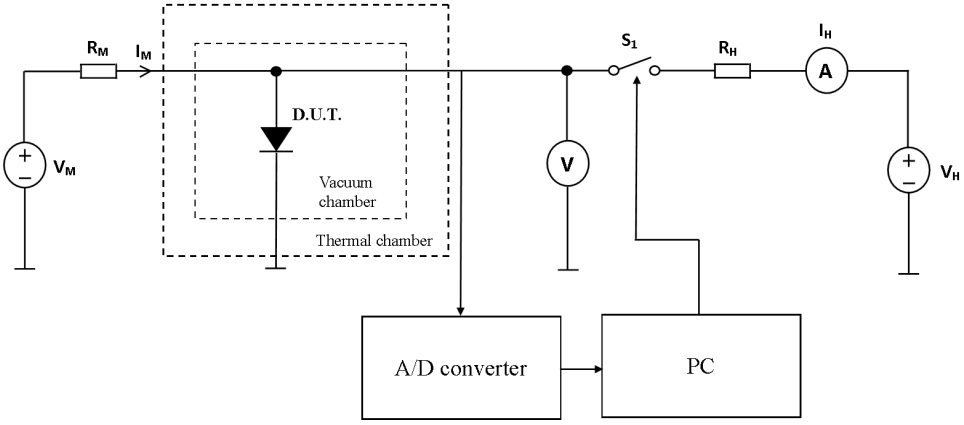

Figure 2. Diagram of the measurement set-up to measure transient thermal impedance of a diode.

The transient thermal impedance measurement using the circuit shown in Figure 2 was performed in four steps:

1. The diode voltage dependence on temperature is measured at a constant value of measurement current I_M. The slope of this characteristic is F. During this measurement step, switch S_1 is open, and the diode is placed in the thermal chamber, which is used to set the value of the temperature. This step is realized at normal pressure.
2. The diode is heated until it reaches the thermally steady state. At the beginning of this step, the pressure in the vacuum chamber is set. After reaching it, the value of the power dissipated in the component is recorded as p_{th}. During measurement, switch S_1 is closed, and current I_H flows through the diode.
3. The waveform $v_D(t)$ of the diode forward voltage is recorded by an A/D converter at a constant value of measurement current I_M from time $t = 0$, at which switch S_1 is opened, until the thermally steady state is obtained.
4. The transient thermal impedance is calculated using the formula

$$Z_{th}(t) = \frac{v_D(t=0) - v_D(t)}{F \cdot p_{th}} \quad (3)$$

The measurement error of thermal resistance using the formulated method is a decreasing power function [25]. Regarding discrete devices placed on a heat sink, the measurement error for the junction temperature equals the permissible value given that the datasheet does not exceed 5% [26].

During the measurements, the diode was placed in a vacuum chamber with a volume of 80 L. The heat sink to which the diode was screwed was placed in the chamber on the big wooden block. In order to force the ambient temperature below room temperature, the vacuum chamber was placed in a Binder UF V (E3) freezer. DM3068 multimeters (Rigol, Portland, OR, USA) were used to measure voltages and currents in the thermally steady state. The circuit was powered from Keithley 2260B-30-36 (Tektronix, Beverton, OR, USA) (V_H) and DF1760SL10A (NDN, Warsaw, Poland) (V_M) sources.

4. Experimental Verification

In order to verify the correctness of the model described by Equation (2), the computations and measurements of the $Z_{thj-a}(t)$ waveforms of the selected diode operating under various operating conditions were carried out. The tested diode was a silicon power diode IDP08E65, with a maximum forward current of 16 A and packed in a TO-220 case. Regarding the devices packed in the TO-220 case, it is common to use cooling systems; therefore, the considered device was tested by placing it consecutively on an aluminum grilled heat sink with dimensions of 75 mm × 50 mm × 35 mm.

This section presents the results of the experimental verification of the formulated thermal model. In order to obtain this goal, $Z_{thj-a}(t)$ measurements of the diode were made in various operating conditions using the measurement set-up presented in the previous section and were compared with the computation results.

The computations were performed for the set of parameters presented in Table 1. These parameters were determined in accordance with the method of estimating the parameters of the compact thermal model presented in [20]. They are based on the results of the measurements of transient thermal impedance of a semiconductor device under steady cooling conditions.

Table 1. Values of the parameters of the thermal model of the tested diode.

parameter	R_{th0} [K/W]	R_{th1} [K/W]	R_{th2} [K/W]	T_z [K]	p_z [hPa]	T_0 [K]	p_0 [hPa]
value	5.5	5.5	0.5	26	315	298	1000
parameter	a [K^{-1}]	b [K^{-1}]	d_4	d_5	R_1 [K/W]	R_2 [K/W]	R_3 [K/W]
value	6×10^{-4}	8.3×10^{-4}	0.716	0.1	0.8	0.92	0.061
parameter	C_1 [J/K]	C_2 [J/K]	C_3 [J/K]	C_4 [J/K]	C_5 [J/K]		
value	0.01247	0.7172	16.86	118.5	5300		

Figures 3–8 show the results of computations (lines) and measurements (points) obtained for different operating conditions of the tested diode.

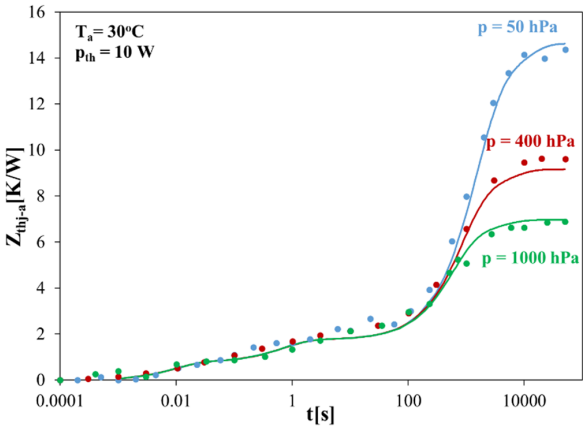

Figure 3. Measured and computed waveforms of transient thermal impedance of the tested diode for three values of atmospheric pressure.

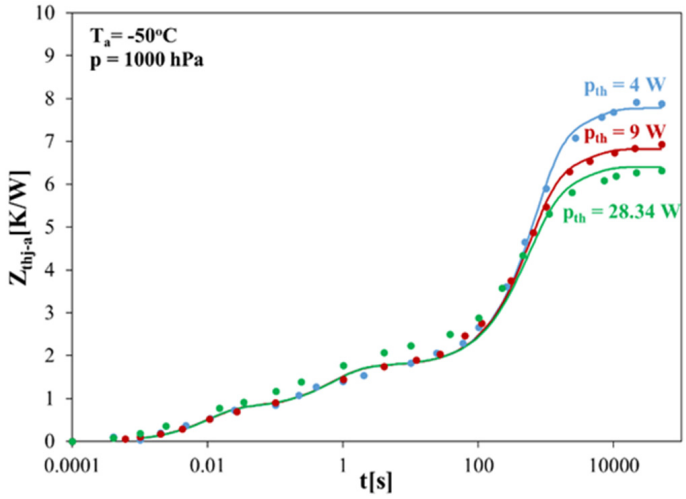

Figure 4. Measured and computed waveforms of transient thermal impedance of the tested diode for three values of dissipated power.

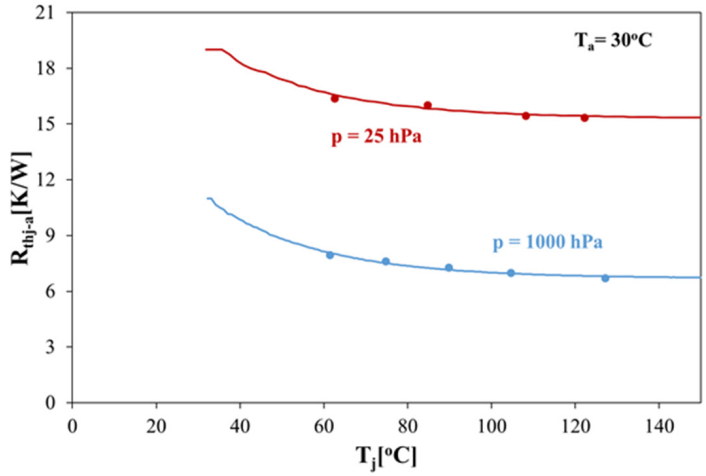

Figure 5. Measured and computed dependences of thermal resistance of the tested diode on the junction temperature for two values of atmospheric pressure.

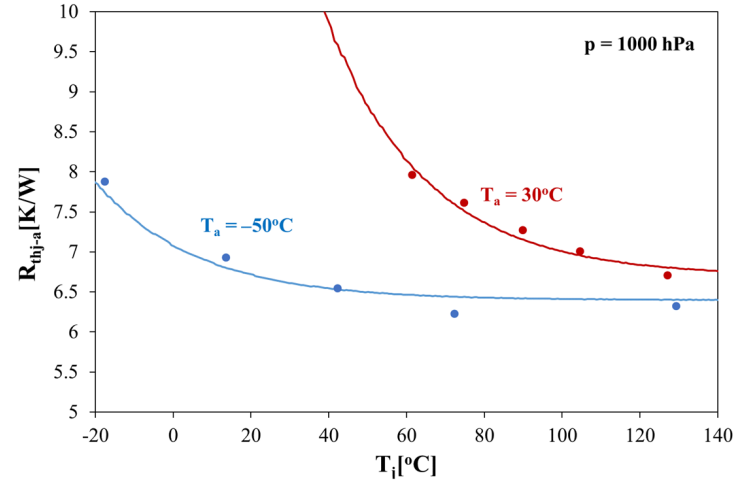

Figure 6. Measured and computed dependences of thermal resistance of the tested diode on the junction temperature for two values of ambient temperature.

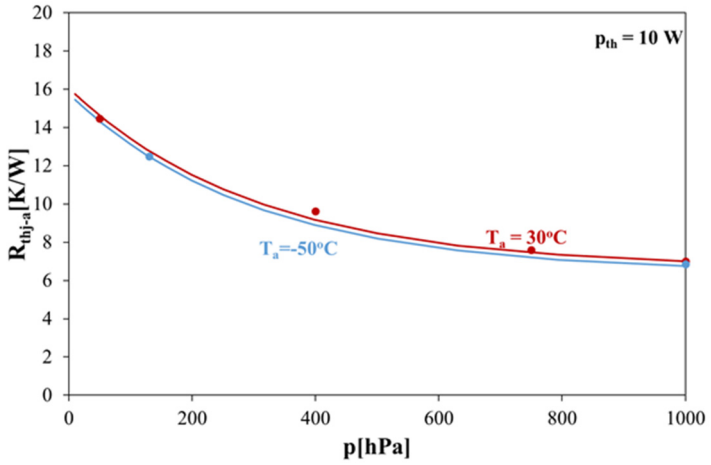

Figure 7. Measured and computed dependences of thermal resistance of the tested diode on atmospheric pressure for two values of ambient temperature.

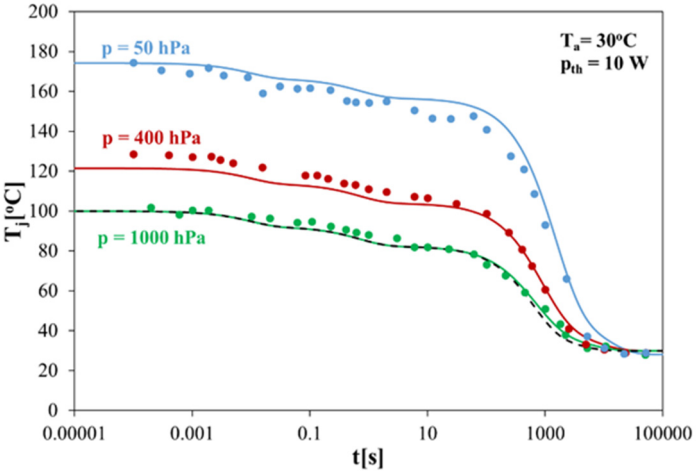

Figure 8. Measured and computed waveforms of the junction temperature of the tested diode for three values of atmospheric pressure.

In Figure 3, the measured and computed waveforms of the transient thermal impedance of the tested diode placed on the heat sink for three values of atmospheric pressure are presented.

According to the measurement results presented in Figure 3, the waveform of transient thermal impedance $Z_{thj-a}(t)$ of the diode placed on the heat sink strongly depends on atmospheric pressure. This dependence is visible for time t above 100 s, which means that it relates to heat dissipation from the heat sink to the surroundings [27]. The components of thermal resistance characterizing this process increase with a decrease in atmospheric pressure due to a decrease in the efficiency of heat convection from the surface of the heat sink [27]. As atmospheric pressure decreases in the studied range of its changes, thermal resistance R_{thj-a} increases by over 100%. The formulated model allows accurate modeling of the influence of atmospheric pressure on the course of the transient thermal impedance of the diode $Z_{thj-a}(t)$. The discrepancy between the results of computations and measurements does not exceed 0.5 K/W.

Figure 4 shows the transient thermal impedance of the diode placed on the heat sink for three different values of the power dissipated in it at normal pressure (p = 1000 hPa) and an ambient temperature of −50 °C.

In the studied power range, according to the data presented in Figure 4, thermal resistance R_{thj-a} decreases by as much as 20%. The formulated model given by Equation (2) allows computing the waveforms of transient thermal impedance $Z_{thj-a}(t)$ with high accu-

racy. Under the considered conditions, the discrepancy between the results of computations and measurements does not exceed 0.4 K/W. The thermal resistance R_{thj-a} of a diode decreases with an increase in the power dissipated in it. This is due to a temperature increase in all the elements of the heat flow path from the semiconductor chip to the surroundings. As a result, the efficiency of the convection mechanism increases, which causes a decrease in the value of thermal resistance [22].

Figure 5 shows the dependence of the diode thermal resistance R_{thj-a} as a function of the interior temperature for two values of atmospheric pressure and the set temperature value T_a = 30 °C.

As can be seen in Figure 5, under the conditions of reduced pressure that is 40 times lower than normal, the thermal resistance for the junction temperature of 150 °C is as much as 130% higher than at p = 1000 hPa. This is due to the reduced efficiency of heat removal from the heat sink at low atmospheric pressure. The effect of such a change in thermal resistance is a significant, more than two-fold reduction in the value of the maximum allowable power dissipated in the tested diode.

Figure 6 shows the dependence of the diode thermal resistance R_{thj-a} on the junction temperature for two values of ambient temperature.

The measured and computed dependences of thermal resistance R_{thj-a} presented in Figure 6 prove that, in order to correctly model the dependence of thermal resistance on temperature, both the ambient temperature and the junction temperature should be considered. The values of thermal resistance R_{thj-a}, with a change in the ambient temperature by 80 °C, may differ by more than 20% for the same value of the junction temperature.

Figure 7 shows the dependence of the diode thermal resistance R_{thj-a} on atmospheric pressure for two values of ambient temperature.

As can be seen in Figure 7, the diode thermal resistance R_{thj-a} is an exponentially decreasing function of pressure. When atmospheric pressure changes from 1000 hPa to 50 hPa, it increases by over 100%. The dependence of thermal resistance R_{thj-a} on the ambient temperature is weak but noticeable.

Regarding the results presented in Figures 5–7, the discrepancy between the results of computations and measurements is at the level of the measurement error of the applied method of transient thermal impedance [26].

In order to assess the practical usefulness of the formulated model, Figure 8 presents the results of computations of the diode junction temperature during its cooling from the moment of switching off for three values of atmospheric pressure. The results obtained with the use of the author's model (colored lines) are compared with the results obtained with the commonly used linear model (black dashed line) and the measurement results (points).

As can be seen from the data shown in Figure 8, the use of a linear thermal model enables accurate computation of the diode junction temperature waveforms for only one atmospheric pressure value equal to normal pressure. When determining an increase in the junction temperature with the use of a linear model for a pressure of 50 hPa, the computation error is as high as 70 °C. Regarding the non-linear model, the greatest discrepancy between the results of computations and measurements for pressure equal to 400 hPa does not exceed 8 °C. This proves the usefulness of the formulated model.

5. Conclusions

This paper presents a compact thermal model of a diode considering the influence of atmospheric pressure, its junction temperature and the ambient temperature. It was shown that a power diode, in its typical cooling conditions, i.e., placed on a heat sink, exhibits significant deterioration of its thermal properties when operating in conditions of reduced atmospheric pressure. The cause of the deterioration of these properties is a decrease in the efficiency of convection from the surface of the diode and the heat sink, which is the dominant mechanism of heat dissipation from the heat sink under normal pressure conditions. On the other hand, as the junction temperature increases, the efficiency of free convection increases, which lowers thermal resistance by up to several dozen percent. As

is presented in Section 4, regarding operation at low ambient temperatures, in the range of high temperatures, no decrease in thermal resistance with increasing junction temperature was observed.

The correctness and accuracy of the formulated model were verified experimentally, confirming its usefulness in a wide range of changes in atmospheric pressure, ambient temperature and junction temperature. The discrepancies between the results of computations and measurements do not exceed a few percent, so they are at the level of the measurement error.

The formulated model may be useful for designers of electronic systems that are to operate in the conditions of reduced atmospheric pressure, e.g., in the stratosphere. Omitting the influence of atmospheric pressure on the thermal properties of semiconductor devices when designing electronic systems to operate in such conditions results in a significant reduction in their life span due to a much higher than expected junction temperature, which follows from Figure 8.

Funding: This project was financed in the framework of the program by the Ministry of Science and Higher Education called "Regionalna Inicjatywa Doskonałości" during the years 2019–2022, project number 006/RID/2018/19, the sum of financing 11,870,000 PLN.

Institutional Review Board Statement: Not applicable.

Informed Consent Statement: Not applicable.

Data Availability Statement: Not applicable.

Conflicts of Interest: The author declares no conflict of interest.

Nomenclature

Symbol	Unit	Explanation
R_{thj-a}	K/W	junction-ambient thermal resistance
$Z_{thj-a}(t)$	K/W	junction-ambient thermal impedance
T_j	K	junction temperature
T_a	K	ambient temperature
p_{th}	W	power dissipated in the tested device
d_i		quotient of thermal resistance of ith element of the heat flow path
T_0	K	reference temperature
R_{th0}	K/W	minimum value of thermal resistance at an ambient temperature equal to the reference temperature T_0
R_{th1}	K/W	maximum change in the value of thermal resistance while changing the device internal temperature and $T_a = T_0$
R_{th2}	K/W	coefficient describing the dependence of thermal resistance on atmospheric pressure
T_z	K	coefficient determining the slope of dependence $R_{thj-a}(T_j)$
p_z	hPa	coefficient determining the slope of dependence $R_{thj-a}(T_j)$
a	1/K	ambient temperature rate of change in R_{th0}
b	1/K	ambient temperature rate of change in R_{th1}
p	hPa	atmospheric pressure
C_i	J/K	thermal capacitance
R_i	K/W	thermal resistance
F	V/K	slope of dependence $V_D(T)$
v_D	V	diode forward voltage

References

1. Pande, D.; Verstraete, D. Impact of solar cell characteristics and operating conditions on the sizing of a solar powered nonrigid airship. *Aerosp. Sci. Technol.* **2017**, *72*, 353–363. [CrossRef]
2. Kayhan, Ö. A thermal model to investigate the power output of solar array for stratospheric balloons in real environment. *Appl. Therm. Eng.* **2018**, *139*, 113–120. [CrossRef]

3. Xiaowei, D.; Guoning, X.; Zhaojie, L.; Ying, M.; Shuai, Z.; Hao, D. Remaining useful life prediction of Lithium-ion batteries of stratospheric airship by model-based method. *Microelectron. Reliab.* **2019**, *100–101*, 113400. [CrossRef]
4. Sun, K.; Li, J.; Liang, H.; Zhu, M. Simulation of a Hybrid Energy System for Stratospheric Airships. *IEEE Trans. Aerosp. Electron. Syst.* **2020**, *56*, 4426–4436. [CrossRef]
5. Patrzyk, J.; Bisewski, D.; Zarębski, J. Electrothermal Model of SiC Power BJT. *Energies* **2020**, *13*, 2617. [CrossRef]
6. Castellazzi, A.; Kraus, R.; Seliger, N.; Schmitt-Landsiedel, D. Reliability analysis of power MOSFET's with the help of compact models and circuit simulation. *Microelectron. Reliab.* **2002**, *42*, 1605–1610. [CrossRef]
7. Codecasa, L.; d'Alessandro, V.; Magnani, A.; Irace, A. Circuit-Based Electrothermal Simulation of Power Devices by an Ultrafast Nonlinear MOR Approach. *IEEE Trans. Power Electron.* **2016**, *31*, 5906–5916. [CrossRef]
8. Daia, Q.; Caoa, L.; Zhanga, G.; Fangb, X. Thermal performance analysis of solar array for solar powered stratospheric airship. *Appl. Therm. Eng.* **2020**, *171*, 115077. [CrossRef]
9. Wang, X.; Li, Z.; Zhang, Y. Model for Predicting the Operating Temperature of Stratospheric Airship Solar Cells with a Support Vector Machine. *Energies* **2021**, *14*, 1228. [CrossRef]
10. Zhang, T.; Geng, S.; Mu, X.; Chen, J.; Wang, J.; Wu, Z. Thermal Characteristics of a Stratospheric Airship with Natural Convection and External Forced Convection. *Int. J. Aerosp. Eng.* **2019**, *2019*, 4368046. [CrossRef]
11. Li, J.; Lv, M.; Tan, D.; Zhu, W.; Sun, K.; Zhang, Y. Output performance analyses of solar array on stratospheric airship with thermal effect. *Appl. Therm. Eng.* **2016**, *104*, 743–750. [CrossRef]
12. Malinowski, M.; Leon, J.I.; Abu-Rub, H. Solar Photovoltaic and Thermal Energy Systems: Current Technology and Future Trends. *Proc. IEEE* **2017**, *105*, 2132–2146. [CrossRef]
13. Yang, X.; Liu, D. Renewable power system simulation and endurance analysis for stratospheric airships. *Renew. Energy* **2017**, *113*, 1070–1076. [CrossRef]
14. Ye, Y.H.; Shi, Y.X.; Cai, N.S.; Lee, J.; He, X.M. Electro-thermal modeling and experimental validation for lithium ion battery. *J. Power Sources* **2012**, *199*, 227–238. [CrossRef]
15. Elsayedab, M.L.; Mesalhy, O.; Kizito, J.P.; Leland, Q.H.; Chowa, L.C. Performance of a guided plate heat sink at high altitude. *Int. J. Heat Mass Trans.* **2020**, *147*, 118926. [CrossRef]
16. Oettinger, F.F.; Blackburn, D.L.; Rubin, S. Thermal Characterization of Power Transistors. *IEEE Trans. Electron Dev.* **1976**, *23*, 831–838. [CrossRef]
17. Diebold, E.J.; Luft, W. Transient thermal impedance of semiconductor devices. *Am. Inst. Electr. Eng. Part I Commun. Electron.* **1961**, *79*, 719–726. [CrossRef]
18. Górecki, K.; Zarębski, J. Modeling the Influence of Selected Factors on Thermal Resistance of Semiconductor Devices. *IEEE Trans. Comp. Packag. Manuf. Technol.* **2014**, *4*, 421–428. [CrossRef]
19. Janicki, M.; Torzewicz, T.; Samson, A.; Raszkowski, T.; Sobczak, A.; Zubert, M.; Napieralski, A. Experimental investigation of discrete air cooled device thermal resistance dependence on cooling conditions. *Microelectron. Reliab.* **2017**, *79*, 405–409. [CrossRef]
20. Górecki, K.; Górecki, P. Nonlinear Compact Thermal Model of the IGBT Dedicated to SPICE. *IEEE Trans. Power Electron.* **2020**, *35*, 13420–13428. [CrossRef]
21. Cheng, T.; Lu, D.D.C.; Siwakoti, Y.P. A MOSFET SPICE Model with Integrated Electro-Thermal Averaged Modeling, Aging, and Lifetime Estimation. *IEEE Access* **2021**, *9*, 5545–5554. [CrossRef]
22. Bagnoli, P.E.; Casarosa, C.; Ciampi, M.; Dallago, E. Thermal resistance analysis by induced transient (TRAIT) method for power electronic devices thermal characterization—Part I, Fundamentals and theory. *IEEE Trans. Power Electron.* **1998**, *13*, 1208–1219. [CrossRef]
23. Yener, Y.; Kakac, S. *Heat Conduction*; Taylor & Francis: New York, NY, USA, 2008.
24. Górecki, K.; Zarębski, J. Nonlinear Compact Thermal Model of Power Semiconductor Devices. *IEEE Trans. Compon. Packag. Technol.* **2010**, *33*, 643–647. [CrossRef]
25. Górecki, K.; Ptak, P. New Method of Measurements Transient Thermal Impedance and Radial Power of Power LEDs. *IEEE Trans. Instrum. Meas.* **2020**, *69*, 212–220. [CrossRef]
26. Górecki, K.; Górecki, P. The Analysis of Accuracy of Selected Methods of Measuring the Thermal Resistance of IGBTs. *Metrol. Meas. Syst.* **2015**, *22*, 455–464. [CrossRef]
27. Janicki, M.; Sarkany, Z.; Napieralski, A. Impact of nonlinearities on electronic device transient thermal responses. *Microelectron. J.* **2014**, *45*, 1721–1725. [CrossRef]